ERROR CHARACTERIZATION AND APPLICATION OF ATMOSPHERIC MOTION VECTORS OVER AUSTRALIA AND HIGH LATITUDES

J. Le Marshall[1, 2] **R. Seecamp**[2] **, A. Rea**[2] **, M. Dunn**[3] **, J. Jung**[4]**, J. Daniels**[5] **and C. Velden**[4]

[1] Joint Center for Satellite Data Assimilation, NOAA Science Center, MD, USA
[2] Bureau of Meteorology, Melbourne, AUSTRALIA
[3] Physics Dept., Latrobe University, Melbourne, AUSTRALIA
[4]Cooperative Institute for Meteorological Satellite Studies, University of Wisconsin, USA
[5]National Environmental Satellite Data Information Services, MD, USA

ABSTRACT

High density atmospheric motion vectors (AMVs) have been used operationally since the middle 1990s. Their benefit to NWP is dependent on quality control, error characterization and data selection. Here, we show that quality control (q.c.) considerably reduces vector error. In some cases, q.c. also reduces the correlated error and its associated length scale. Modern operational data assimilation schemes require estimates of observation errors, and they assume that the errors are uncorrelated or require knowledge of their correlated error and length scale. The expected error (EE) is now generated at the Australian Bureau of Meteorology (ABM), in addition to QI, RFF and other error indicators, to aid in quality control and error characterization of AMVs for numerical weather prediction (NWP). Provision of the correlated error and length scale also provides a firm basis for data thinning.

Error characterized and quality controlled AMVs have recently been used in a data assimilation experiment to gauge the impact of locally generated GOES-9 AMVs on operational NWP over the Australian Region. Their clear benefit is shown. These vectors are now being used in NMOC for operational NWP. In another recent experiment AMVs generated from sequential MODIS images at high latitudes have also been used in a data impact study to demonstrate their utility in global NWP.

1. INTRODUCTION

Since the operational use of local AMVs by the ABM began in 1992 (Le Marshall et al. 1992), it has been known that careful q.c. of the winds is required to ensure a positive impact in regional and global data assimilation. Their "optimal" use is dependent on the characterization of errors associated with particular vector types. During production, vectors with unacceptably large (gross) errors are typically removed by examining the temporal consistency of the vectors (the acceleration check), the spatial consistency of the vectors (buddy checks) and by error estimates, based on comparison with the forecast model background field. (Le Marshall et al. 1994, 2002). The AMVs are expected to have spatially correlated errors because of the methods used in their generation and q.c.. For example, errors in image navigation can give rise to spatially correlated velocity errors. A forecast background field with spatially correlated errors is often also used for cloud and water vapour feature height assignment and can lead to correlated errors. Correlated error may also be produced by similar errors in height assignment of fleets of vectors associated with a given cloud area of uniform type. In such cases, height assignment and q.c. are both dependent on a forecast model with correlated errors. Determining these gross and correlated errors is crucially important in data assimilation and NWP.

Here, we examine the q.c., error characterization and assimilation of atmospheric motion vectors and demonstrate that the judicious application of q.c. and error estimation can improve the accuracy and error characterization of the AMVs. Subsequently we examine the effects of quality controlled AMVs from GOES-9 on operational NWP in the Australian Region and we report on the impact of AMVs derived from sequential MODIS imagery at NWP high latitudes.

2. QUALITY CONTROL AND ASSIMILATION

Error determination and rejection in most real time AMV estimation systems are generally based on several elements. These include the correlation between the brightness temperature arrays of the search and target areas, the difference in meridional and zonal wind components of the two vectors from a tracer tracked in adjacent pairs of images, and the deviation of the calculated wind vectors from the first guess field.

For data assimilation, data thinning is also required when using high density AMVs. In practice, thinning is achieved by reducing data density to a separation suggested by the Length Scale of the Correlated Error (typically around 100 km). This is usually achieved by preferentially selecting vectors of higher accuracy. The selection generally involves use of the Quality Indicator (QI), Expected Error (EE), Recursive Filter Flag (RFF), Error Flag (ERR) or other indicators of error level available with the vectors, and should result in an observational error level close to that of the background field. The error levels of the data to be assimilated are generally chosen to be close to or lower than the background errors, particularly away from conventional observations, thereby facilitating improved prognosis. It is also important in the analysis process to also exercise judicious quality control (such as gross error checks) to prevent poorly characterised vectors degrading the analysis.

3. THE QUALITY INDICATOR

The Quality Indicator (QI), has recently been introduced to assist in data selection (Holmlund, 1998) and Holmlund et al. (2001). The QI is associated with each AMV in the BUFR product from EUMETSAT and NESDIS. The QI for each AMV is calculated by estimating direction consistency, speed consistency, vector consistency, spatial consistency and consistency with the operational forecast. The degree of compliance with these five tests is then used to form a single QI. The QI has been beneficial in the application of high-density winds, by providing a consistent estimation of the comparative accuracy associated with each vector. It is an essential error indicator for analysis using Global Telecommunication System (GTS) AMV BUFR data. The QI is also provided for all AMV types generated at the Bureau of Meteorology, using methods similar to those of Rohn et al. (1998) but without the additional (filter) checks now employed by EUMETSAT. Figure 1 is a plot of QI against RMS difference between low level infrared AMVs and radiosondes located within 150 km, using the one year period April 2000 – April 2001. The use of the QI for data selection and error estimation can be improved further by combining it with other quality measures such as the Recursive Filter Flag (RFF) (Holmlund et al., 2001). Note that, if QI is used rather than an *expected error*, then calibration curves similar to those of Fig. 1 need to be estimated for each vector type, for each wind producer.

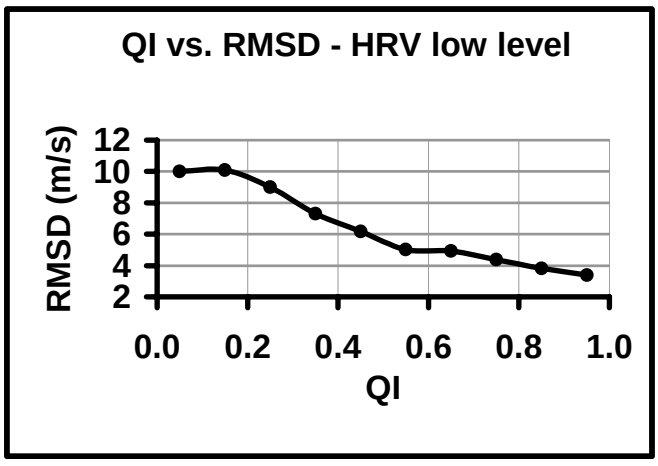

Fig. 1. Quality Indicator (QI) versus root mean square difference (RMSD) with radiosondes within 150 km for low level GMS-5 infrared image based AMVs for 28 April, 2000 to 29 April 2001

4. THE EXPECTED ERROR

The Expected Error (EE), (Le Marshall et al. 2004) is calculated from the wind speed components, the wind shear, the pressure and the elements that make up the QI. The elements of the QI have traditionally been used for q.c. of AMVs since the early 1980s and wind speed is known to be strongly related to AMV error. The vertical wind shear is also clearly related to AMV error, determining how height assignment errors influence AMV quality. Currently, least square regression is used operationally to compute the root mean square error in metres per second (ms^{-1}) from the EE components. Figure 2 (a) is a plot of the error calculated from the QI via a lookup table such as in Fig. (1). Figure 2 (b) is a plot of the EE versus measured error. As suggested from a comparison of Fig. 2 (a) and 2 (b), the EE is on average a more accurate means of determining the observed error.

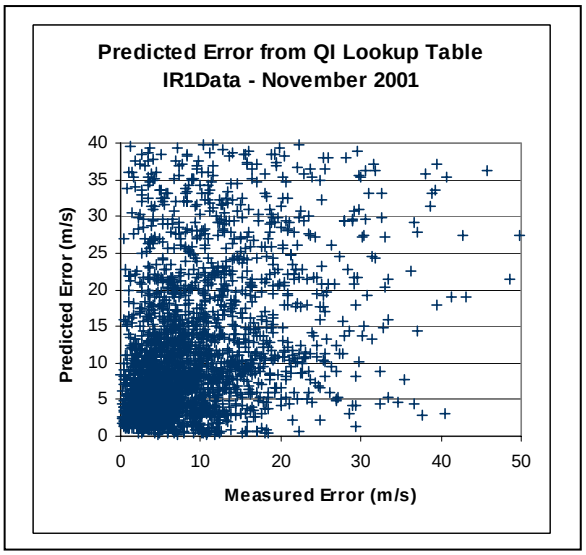

Fig. 2 (a): Predicted error using the QI lookup table.

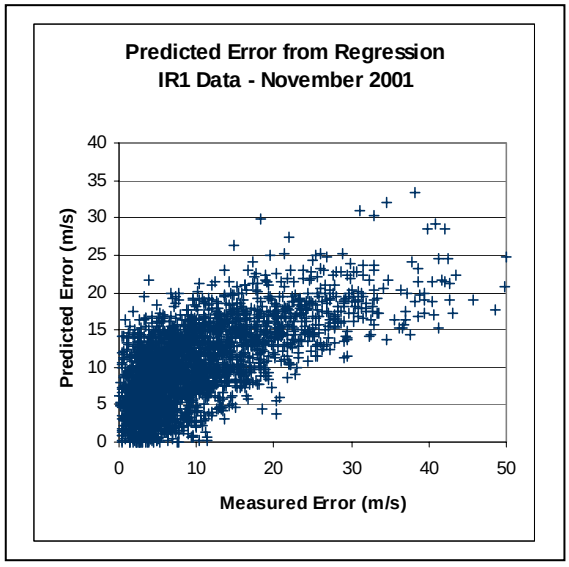

Fig. 2 (b): Predicted error using the EE approach.

Table 1 further summarizes the results. In practice, the EE is also more efficient at data selection, for example, it provides well over 50% more vectors below threshold error levels typical of operational data rejection and also well over 50% more vectors at error levels associated with the background field.

Selection Method	**EE**	**QI**	**EE**	**QI**
Threshold	EE<5.2	QI>.98	EE<8.5	QI>.89
No. of Matches	3156	514	7265	2863
Av. MMVD	5.00	5.00	6.0	6.0
Av. Error in MMVD	3.17	5.24	3.25	4.31

Table 1 AMV numbers and comparative errors in MMVD when selecting Upper level WV AMVs by MMVD (November, 2002) using EE and QI. (Here vector populations are chosen to have Av. MMVD equal to 5 and 6 ms^{-1} respectively).

The improved coverage for a given error level or, equivalently, decreased error levels for the same AMV numbers, *provides an improved basis for analysis and prognosis*. This result is expected as the weights used in EE have been determined specifically to predict the root mean square error whereas those used in the QI were not. Other important aspects of the EE are that it can be used to compare AMVs from different producers and that it can be used quantitatively in conjunction with the correlated error and associated length scale in the analysis process. Figures 3 (a) and 3 (b) are examples showing the QI and EE for AMVs over the Coral Sea on November 7, 2002.

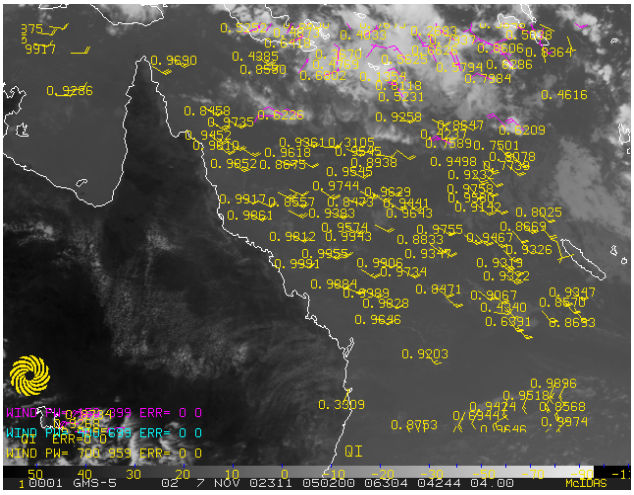

Fig. 3 (a) The QI generated for AMVs over the Coral Sea on 7 November 2002

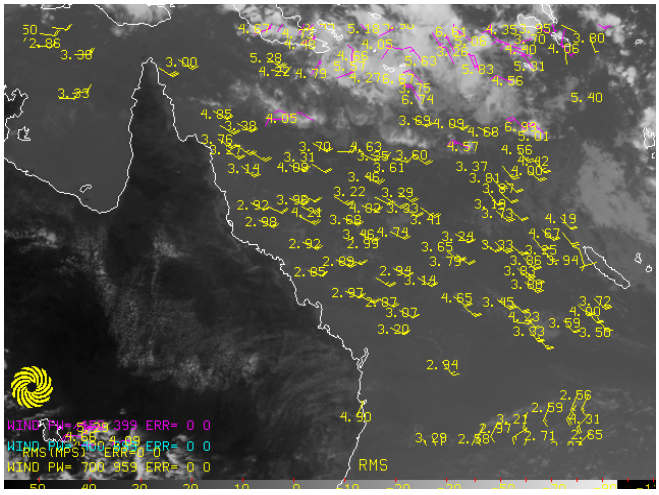

Fig. 3 (b) The EE generated for AMVs over the Coral Sea on 7 November 2002

5. CORRELATED ERROR

In addition to the Expected Error, a Correlated Error (CE) and a length scale (L) are associated with the vectors at the Bureau. The CE has been computed using collocated, contemporaneous radiosonde and AMV observations from a match file. The approach used to derive the spatial variation of correlated error from the match file assumes that the observation errors from radiosondes are spatially uncorrelated. In this case, any observed correlation between the AMV and radiosonde differences in the U or V wind components is attributed to spatially correlated AMV errors. Grouping errors, associated with radiosonde/AMV pairs at the same time, by using separation distance allows a characterization of the average spatial structure of correlated errors for local GMS-5 AMVs. The method has been used widely and was discussed by Daley (1993). Extrapolation of the CE versus distance relationship to zero separation gives the magnitude of the spatially correlated AMV errors. The correlation function provides an estimate of the length scale of the CE. This length scale has been used as a basis for thinning appropriate in regional data assimilation.

The observed data has been analyzed assuming an isotropic error correlation versus distance function, which is satisfactory for an initial application to data assimilation. The correlation function used to extrapolate to zero separation is the second order auto-regressive (SOAR) function (Daley, 1993).

$$R(r) = R_{00} + R_0\left(1+\frac{r}{L}\right)e^{\frac{-r}{L}} \qquad \textbf{(1)}$$

where R(r) is the error correlation, with fitting parameters R_{00}, R_0 (greater than 0), and L is the length scale, 'r' is the separation of the correlates.

Figure 4 and Table 2 show error correlation versus distance for local GMS-5 for AMVs in the Australian Region. Figure 4 (a) shows Error Correlation versus Distance for high level WV vectors derived using 10 km distance separation category bins. The two distributions are for all vectors generated and those selected on error characteristics for use in operational NWP (Ops) in the Bureau. Figure 4 (b) shows the same plot using 100 km separation for the bins. The effect of loss of resolution from binning is just discernible in the second distribution which is smoothed compared to that in Fig. 4 (a). Figures 4 (a) and 4 (b) show a reduction in CE and Length Scale from the quality control associated with the selection of vectors for use in the Bureau's operational regional data assimilation system. A similar reduction in CE Length Scale has also been noted through application of the QI and EE in data selection.

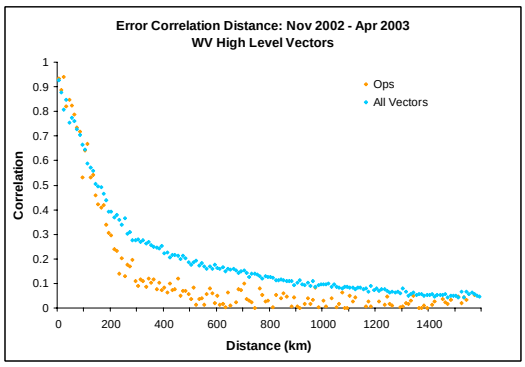

4 (a) Error Correlation versus distance (10 km bins) for all High Level WV AMVs generated and those selected for NWP use (Ops)

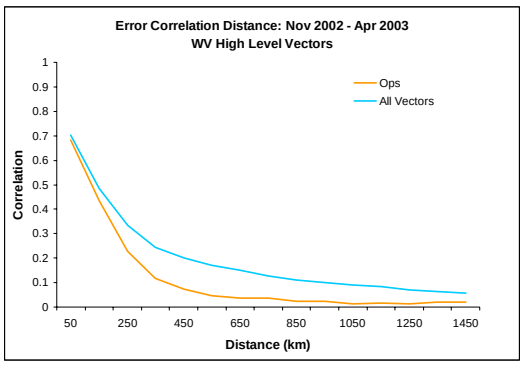

4 (b) Error Correlation versus distance (100 km bins) for all High Level WV AMVs generated and those selected for NWP use (Ops)

The parameters of the SOAR functions fitted to the distance correlation functions for GMS-5 IR1, HRVIS and WV image based AMVs are seen in Tables 2 (a) and 2 (b) which provide R_0, L, CE and root mean square difference (RMSD) compared to radiosondes using CGMS criteria, for non-zero and zero R_{00}.

	R_{00}		R_0		L (km)		Corr. Error (ms^{-1})		RMSD (ms^{-1})	
Level	Low	High	Low	High	Low	High	Low	High	Low	High
IR1	0.04	0.06	0.82	0.83	123.3	73.1	3.23	5.21	3.94	6.28
HRVIS	0	0.01	0.96	0.70	127.2	82.9	3.54	3.82	3.69	5.46
Level	Mid	High	Mid	High	Mid	High	Mid	High	Mid	High
WV	0	0.02	0.67	0.91	95.1	84.8	3.49	4.39	5.21	4.82

Table 2 (a) Parameters of the SOAR function (Equation 1) which best model the measured error correlations for the AMV types listed in the left-hand column

	R_{00}		R_0		L (km)		Corr. Error (ms^{-1})		RMSD (ms^{-1})	
Level	Low	High	Low	High	Low	High	Low	High	Low	High
IR1	0	0	0.84	0.82	141.4	94.3	3.31	5.15	3.94	6.28
HRVIS	0	0	0.96	0.70	127.8	85.1	3.54	3.82	3.69	5.46
Level	Mid	High	Mid	High	Mid	High	Mid	High	Mid	High
WV	0	0	0.51	0.92	95.1	88.9	3.49	4.43	5.21	4.82

Table 3 (b) Parameters of the SOAR function (Equation 1) which best model the measured error correlations for the AMV types listed in the left-hand column. R_{00} is assumed to be zero.

The above analysis shows length scales (L) to be larger at lower levels in this data set. Upper length scales for a given R_{00} are similar while, at lower levels, HRVIS displays a larger length scale than those for IR1 and WV. In comparison with the lower resolution statistics (100 km bins) of Bormann et al. (2003), the length scales here are shorter and CE and R_0 are larger, a result aided by 10 km bins. Note that, in this study. lower level vectors appear to have a larger average L and vectors selected via error using QC and EE (higher quality vectors) for NWP use, have shorter average length scales associated with their CE.

6. APPLICATION OF GOES-9 AMVs

GOES-9 was moved along the Equator to 155° E, 0° S in 2003 and has been operated over the Western Pacific, Asia and the Australian Region as the primary geostationary meteorological satellite by the joint effort of JMA and NOAA/NESDIS. Since 22 May 2003, GOES-9 GVAR data have been received via direct readout by the ABM and the calibrated and navigated radiance data (imagery) has subsequently been used

to calculate AMVs. These operational AMVs are important to Australian region NWP as no other AMV data are available within operational cut-off times. The method used to determine atmospheric motion differs from that usually employed for GOES series satellite data, particularly in height assignment, error characterization and q.c. The AMV data have been used in a real time trial to gauge their impact on operational regional Numerical Weather Prediction (NWP). Their clear benefit is described below. As a result of this trial these vectors are now being used in the National Meteorological and Oceanographic Center (NMOC) for operational regional NWP.

7. GOES-9 ATMOSPHERIC MOTION VECTORS

After GOES-9 replaced GMS-5, methods related to those employed at NESDIS (Daniels et al. 2000) and also at the ABM (Le Marshall et al. 2000) have been used to determine AMVs from GOES-9 GVAR data received at the ABM's groundstation at Crib Point. In this system, target selection commence with a search for tracers in the11µm (channel 4) infrared images using bidirectional brightness temperature gradients in 15 x 15 pixel boxes. Gradients are examined to ensure that cloud edges are being tracked. Prospective targets are subjected to a spatial coherence analysis (Coakley and Bretherton, 1982) and then tracked using a lagged correlation technique. After the tracers are selected, the three sequential GOES-9 infrared images are carefully navigated using matching of land features. The height assignment method used for upper level AMVs is similar to on Nieman et al. (1993). The technique employed is the H_2O-intercept method, using 11 µm (channel 4) observations and the 6.7 µm (channel 3) observations. Radiances from the infrared and water vapour channels are measured and compared to calculate Planck blackbody radiances as a function of cloud top pressure. The cloud top altitude is then inferred from a linear extrapolation of radiances onto the calculated curve of opaque cloud radiances, providing the target altitude. The temperature profile used in this process comes from the operational regional forecast model. No subsequent adjustment (autoediting) of the vector altitude occurs for GOES-9 AMVs to make them more consistent with the information in the forecast field guess fields.

The low-level AMV altitude assignment technique is similar to that developed in the ABM (Le Marshall et al. 2000) where cloud altitude is assigned to the cloud base for low-level vectors. No subsequent adjustment (autoediting) of the vector altitude occurs for GOES-9 AMVs to make them more consistent with the information in the forecast first guess fields.

An example of the wind observations generated around 22 UTC on 2 July 2003 in the Australian Region is seen in Fig. 5.

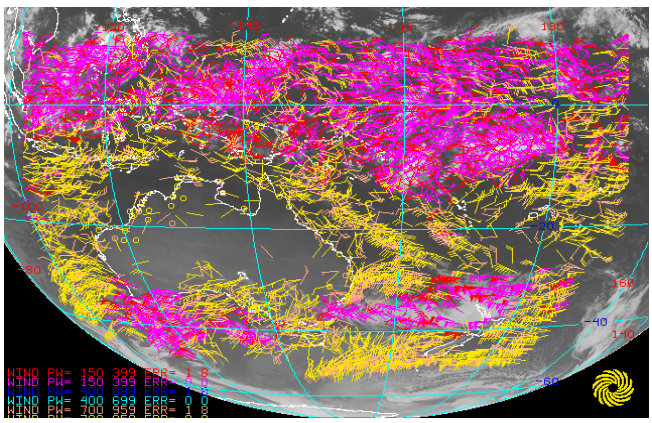

Fig. 5 A selection of GOES-9 AMVs calculated around 22 UTC on 2 July 2003. Magenta denotes upper level tropospheric vectors (above 500 hPa), yellow lower level tropospheric vectors (below 500 hPa)

The AMVs used in this study have been quality controlled using a variety of tests. A local error index (ERR), the Quality Indicator QI, the RFF and RFI (Holmlund et al. 2000) and the Expected Error (Le Marshall et al. 2004) are generated for each GOES-9 AMV and used in quality control and error estimation. Using this information the winds are effectively thinned by quality measure to ensure good data coverage with average separations around the length scale of the correlated error (see Bormann et al. 2003, Le Marshall et al. 2004). The thinning methodology and quality control result in errors not significantly larger than the background error of the forecast model, measured at radiosonde sites. The approach used is detailed in Le Marshall et al. (1994, 2004).Table 3 gives the Mean Magnitude of Vector Difference between GOES-9 AMVs and radiosondes winds within 150 km in the Australian Region for 9 June to 30 June 2003, the period used for the data assimilation experiment.

GOES-9	No. Obs	MMVD (ms^{-1})
Low 950 – 700 hPa	431	3.64
Middle 699 – 400 hPa	82	4.00
High 399 – 150 hPa	1759	4.58

Table 3 Mean Magnitude of Vector Difference (MMVD) between GOES-9 AMVs and radiosondes winds within 150 km in the Australian Region for 9 June to 30 June 2003

8. THE OPERATIONAL TRIAL

8.1 The Assimilation System

The assimilation methodology employed the real time operational NMOC regional Limited Area Prediction System (Puri et al. 1998), using all available data (including JMA winds which were available for the second last analysis in the cycle) *as the control*. The analyses on which the forecasts reported here are based start with a Bureau global analysis (Seaman et al. 1995), valid 12 hours prior to the forecast start time. This is used as a first guess to the regional analysis which then provides the base analysis for an initialized six hour forecast, a subsequent analysis and a further initialized six hour forecast. This forecast is then used as a first guess to the final analysis from which the 24 and 48 hour forecasts are run. Forecasts are nested in fields from the most recent Bureau global model forecast (Bourke et al. 1995).

8.2 Method

GOES-9 AMVs generated using 11 µm (Ch. 4) and 6.7 µm (Ch. 3) images were added to the operational regional assimilation system. The methodology was similar to that used in Le Marshall et al. (2002). The accuracy of real time AMVs provided to the assimilation system for use in this experiment in mid-2003 is summarized in Table 3. Local quality control (Le Marshall et al. 2002) methods were used to provide vectors with expected error consistent with the error levels expected for AMVs in the operational analysis for low, middle and high level vectors, respectively.

A series of parallel *real time* forecasts were run using the operational forecast system as the control. The difference between operational and experimental real time systems was that local GOES-9 AMVs were added to the data base in the experimental system. The experimental period was from 00 UTC on 9 June to 00 UTC on 30 June 2003 (36 cases). The experimental period was not overly long but encompassed a wide variety of synoptic patterns in the Australian Region from zonal flow to highly unusual blocking sequences, including a Tasman Sea cut-off low.

8.3 Results

The S1 skill (Teweles and Wobus, 1954) scores for 24-hour and 48-hour forecasts from using GOES-9 AMV data are compared to the operational skill scores in Table 4. The statistics are consistent with those recorded in earlier impact studies with GMS-5 (Le Marshall et al. 2003).

LEVEL	(LAPS) S1		(LAPS + GOES-9 AMVS) S1	
	24-hr. forecast	48-hr. forecast	24-hr. forecast	48-hr. forecast
MSLP	19.6	30.1	18.6	29.5
850 hPa	16.6	27.5	16.4	26.5
500 hPa	14.1	22.2	13.8	21.5
300 hPa	12.3	18.9	12.1	18.5

Table 4. 24 hr forecast verification (S1) for the operational regional forecast system (LAPS) and LAPS with GOES-9 based AMVs for 9 June to 30 June 2003 (36 cases)

The results from this real time experiment are also illustrated in Figs. 6 to 8. Fig. 6 shows a plot of the operational skill scores versus the skill scores from the operational system with GOES-9 AMVs in its database. Points below the diagonal indicate an improvement in accuracy. It can be seen that a clear majority of points lie below the line and, in particular, that most improvement occurs at the higher values of the S1 Skill Score, i.e. in the lower atmospheric levels for poorer forecasts.

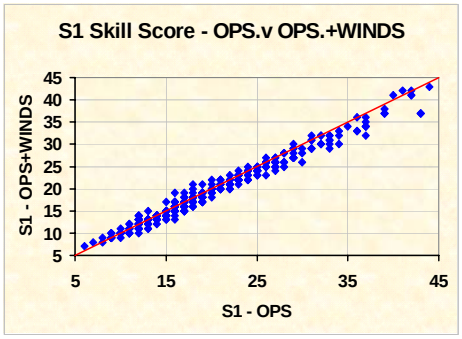

Fig. 6. The S1 Skill Score from Ops. Versus the S1 from Ops. plus GOES-9 winds, 9 June to 30 June 2003.

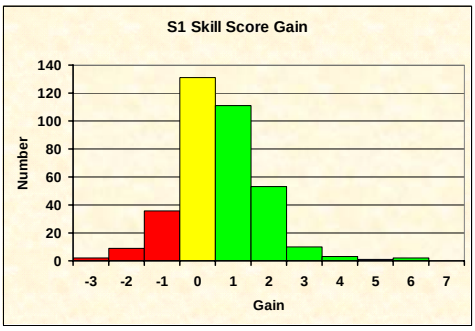

Fig. 7. A histogram of S1 Skill Score gains for 24-hour and 48-hour forecasts at standard model levels, 9 June to 30 June 2003.

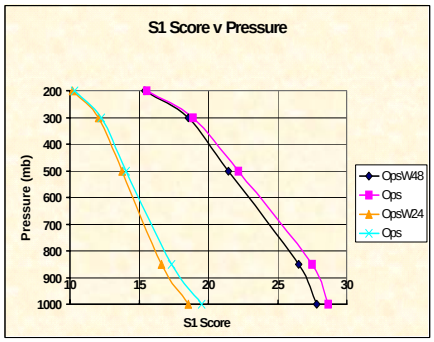

Fig. 8. The S1 Skill Score versus Pressure for real time 48-hour forecasts (right hand pair) and 24-forecasts during the period 9 June to 30 June 2003.

A histogram, giving a summary of the skill score impact is also seen in Fig. 7. The red columns indicate negative impact, yellow neutral impact and green positive impact. Clearly, the positive green impacts dominate the plot. The last plot, Fig. 8, shows the S1 Skill Score versus Pressure Level for 48-hour (right hand pair) and 24-hour (left hand pair) real time forecasts. It shows that the addition of these data has improved the real time forecast at all levels at all times with greater impact in the lower troposphere. Overall, it is clear these winds are beneficial to the forecast process.

In summary, we have shown that real time GOES-9 IR and WV image based AMVs, are of an accuracy which can benefit operational NWP in the Australian Region. Addition of the vectors to the operational regional forecast system has provided both improved data coverage of the region and forecast improvement. *The winds have been used in NMOC, Melbourne, since early August 2003, in the operational regional forecast system.*

9. APPLICATION OF MODIS POLAR AMVs

Winds generated by NOAA NESDIS, (Daniels et al., 2004) using sequential observations from the MODIS instruments on the TERRA and AQUA satellites in the IR and the Water Vapour absorption band have been assimilated into the operational NCEP (3DVAR) Global Forecast System to gauge their impact on the current operational system. The period examined was during the International MOWSAP (MODIS Winds Special Acquisition Period), namely 1 January to 15 February 2004. This was an important test for the NESDIS MODIS AMV system used to generate these winds, as this system will provide these data operationally for the international community.

This global assimilation study used MODIS Wind data up to the second last analysis in the cycle. This was done as the current operational availability of the wind data in relation to the NCEP operational cut-off times namely 2¾ hours. The study demonstrated these, data can improve NCEPs forecasts.

A diagram showing the impact of the wind data on Global Model Forecasts at three days is seen in Fig. 9. It shows most benefit occurs where the extra wind data ameleorates the problem of poor forecasts (i.e. reduces the extent of the downward pointing spikes (forecast busts).)

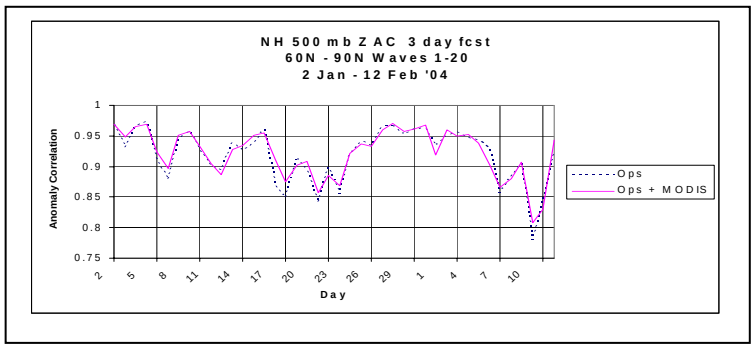

Fig. 9 Three day global forecast accuracy (anomaly correlations) at 500hPa for NCEP Operations and Operations plus MODIS AMVs.

Further quantification of this impact is continuing and it is anticipated these data will be included in the Operation Forecast Suite during the next system upgrade at NCEP.

10. SUMMARY AND CONCLUSIONS

In this study we have described methods used by the ABM in the production, q.c. and error characterization of local AMVs and have demonstrated that q.c. and error characterization are vital components of the AMV generation process. A new method of error characterization, the Expected Error (EE) which provides the error associated with each AMV has been noted. The method predicts the errors associated with AMVs more accurately than other methods in common use. Use of the EE results in improved data coverage at a given error level or the same data numbers with improved accuracy. In addition, the estimated error (EE) of each vector can be used directly in the analysis process and all AMVs can be treated in a similar fashion. Moreover, there is no need for all users to derive, or to receive QI calibration curves for each producer and for each wind type. The characteristic length scale (L) and correlated error (CE) have also been estimated and allow AMVs to be characterized by EE, QI, RFF and also their CE and L. The EE, R_0 and L can be used directly in the analysis process.

The local estimation of real time operational GOES-9 AMVs and their impact on regional NWP has also been described. Experiments using these data in a real time NWP trial have been summarized. The clear benefit of these data to operational regional NWP has been recorded. These results have led to the introduction of these winds into NMOC's operational database and their use in operational regional NWP since August 2003. A recent experiment using MODIS AMVs over high latitudes has also been described. The positive impacts recorded over northern and southern high latitudes have led to these winds being accepted for inclusion in the operational data base at the next operational upgrade at NCEP.

Looking ahead, the continuing trend to space-based observations with higher spatial, temporal and spectral resolution should enable improved estimation of atmospheric motion and result in quantitative benefit to NWP. In particular, the prospects of significant benefits from the use of sequential observations from MTSat-1R, which will have similar observational capability to GOES-9 and new generation ultra-spectral instruments such as the Geostationary Imaging Fourier Transform Spectrometer (Smith et al. 2000) are very good.

ACKNOWLEDGEMENTS: Thanks are due to A. Armstrong, T. Adair and I. Mouzouri for their help in preparing this manuscript. One of us (MD) acknowledges the support of an Australian Postgraduate award and a Victorian Government Information and communication Technologies Postgraduate Scholarship.

REFERENCES

Borrmann, N., S. Saarinen, G. Kelly and J-N. Thépaut. 2003. The spatial structure of observation errors in atmospheric motion vectors From geostationary satellite data. *Mon. Wea. Rev.* **131**, 706 – 718.

Bourke, W.P., Hart, T., Steinle, P., Seaman, R., Embery, G., Naughton, M. and Rikus, L. 1995. Evolution of the Bureau of Meteorology's Global Assimilation and Prediction System. Part 2 : Resolution enhancements and case studies. *Aust. Meteor. Mag.* **44**, 19 - 40.

Coakley, J. and F. Bretherton. 1982. Cloud cover from high resolution scanner data : Detecting and allowing for partially filled fields of view. *J. Geophys. Res.* **87**(C7), 4917 – 4932

Daley, R. 1993. Atmospheric data analysis. Cambridge University Press, Cambridge, UK, 460 pp.

Daniels, J., Velden, C., Busby, W. and Irving, A. 2000. Status and Development of Operational GOES Wind Products. *Proc. Fifth International Winds Workshop, Lorne, Australia, 28 – 31 March 2000*. Published by EUMETSAT EUM P28 ISSN 1023-0414. 27 – 45.

Daniels et al., 2004 from Le Marshall et al. Daniels, J., Velden, C., Bresky, N. and Irving, A., 2004; Status of the NOAA/NESDIS Operational Satellite Wind Product System: Recent Improvements, New Products, Product Quality, and Future Plans. Proceeding of the Seventh International Winds Workshop 1-17 June 2004, Helsinki. (EUMETSAT)

Holmlund, K. 1998. The utilization of statistical properties of satellite-derived atmospheric motion vectors to derive Quality Indicators. *Weath. Forecasting* **13**, 1093 - 1104.

Holmlund, K., Velden, C. and Röhn., M. 2001. Enhanced automatic quality control applied to high-density satellite derived winds. *Mon. Wea. Rev.* **129**, 517 – 529.

Le Marshall, J.F., Pescod, N.R., Mills, G.A. and Stewart, P.K. 1992. Cloud drift winds in the Australian Bureau of Meteorology: An operational note. *Aust. Meteor. Mag.* **40**, 247 - 250.

Le Marshall, J**.**F., Pescod, N., Seaman, R., Mills, G. and Stewart, P. 1994. An operational system for generating cloud drift winds in the Australian Region and their impact on numerical weather prediction. *Wea. Forecasting,* **9**, 361 - 370.

Le Marshall, J.F. Pescod, N. Seecamp, R. Rea, A. Tingwell, C. Ellis, G. and H. Shi. 2000. Recent advances in the quantitative generation and assimilation of high spatial and temporal resolution satellite winds*. Proceedings of the Fifth International Winds Workshop. Lorne, Australia, 28 – 31 March, 2000. 47 – 56. Published by EUMETSAT EUM P28. ISSN 1023-0414.*

Le Marshall, J.F. Leslie L.M. Seecamp, R. 2003 High Resolution Space based wind observations. Estimation and application – A review. Mausam Paper **54**, 1 - 12.

Le Marshall, J**.**, G. Mills, N. Pescod, R. Seecamp, K. Puri, P. Stewart, L.M. Leslie, and A. Rea. 2002. The estimation of high density atmospheric motion vectors and their application to operational numerical weather prediction. *Aust. Meteor. Mag.* **51**, 173 – 180.
Le Marshall, J., A. Rea, L. Leslie, R.Seecamp and M. Dunn. 2004. Error Characterization of Atmospheric Motion Vectors. *Aust. Meteor. Mag.,* **53**, 123 – 131.

Nieman, S., Schmetz, J. and Menzel, W.P. 1993. A comparison of several techniques to assign heights to cloud tracers. *J. Appl. Meteor.* **32**, 1559 – 1568.

Puri, K., Dietachmeyer, G., Mills, G.A., Davidson, N.E., Bowen, R.M. and Logan L.W. 1998. The new BMRC Limited Area Prediction System, LAPS. *Aust. Meteor. Mag*. **47**, 203 - 223.

Röhn, M., Kelly, G. and Saunders, R. 1998. Transition to cloud motion winds from Meteosat with 90 minute sampling and the use of the MPEF quality indicator. *EUMETSAT/ECMWF Research Report No. 7*.

Seaman, R., Bourke, W., Steinle, P., Hart, T., Embery, G., Naughton, M. and Rikus, L. 1995. Evolution of the Bureau of Meteorology's Global Assimilation and Prediction system. Part 1 : analysis and initialisation. *Aust. Meteor. Mag*. **44**, 1 - 18.

Smith, W.L., Harrison, F.W., Revercomb, H.E., Bingham, G.E., Huang H.L. and Le Marshall, J.F. 2000. The Geostationary Imaging Fourier Transform Spectrometer. *Proc. Eleventh International TOVS Study Conference, Budapest, Hungary.* 391 - 398.

Teweles, S. and Wobus, H. 1954. Verification of Prognostic Charts. *Bull. Amer. Meteor. Soc.* **35**, 455 - 463.